

Theory of Interacting Parallel Quantum Wires

Yinlong Sun and George Kirczenow

Department of Physics, Simon Fraser University, Burnaby, BC, Canada V5A 1S6

Phone: (604) 291-2502 or (604) 574-3848, Fax: (604) 291-3592

E-mail: sun@sfu.ca or kirczeno@sfu.ca

Index number: 7335 Mesoscopic systems

arXiv:cond-mat/9502046v3 14 Feb 1995

ABSTRACT

We present self-consistent numerical calculations of the electronic structure of parallel Coulomb-confined quantum wires, based on the Hohenberg-Kohn-Sham density functional theory of inhomogeneous electron systems. We find that the corresponding transverse energy levels of two parallel wires lock together when the wires' widths are similar and their separation is not too small. This energy level locking is an effect of Coulomb interactions and of the the density of states singularities that are characteristic of quasi- one-dimensional Fermionic systems. In dissimilar parallel wires level lockings are much less likely to occur. Energy level locking in similar wires persists to quite large wire separations, but is gradually suppressed by inter-wire tunneling when the separation becomes small. Experimental implications of these theoretical results are discussed.

I. INTRODUCTION

Nanostructures fabricated from semiconductor heterostructures have stimulated many studies in recent years. [1] Various techniques [1,2] such as electron-beam lithography, ion-beam exposure, and etching have been developed to confine the two-dimensional electron gas (2DEG) in heterostructures so as to form quantum wires and constrictions with characteristic dimensions on the 100 nm scale. There have been many theoretical studies of the electronic structure of single quantum wires [3,4,7,6–9]. For multiple parallel wires, theoretical studies of transport in models of non-interacting electrons [10,11] and interacting electrons [12] have been published, and electronic structure calculations of coupled quantum wires have also begun to appear [13,14]. Recently, it has been demonstrated [14], using the density functional theory of Hohenberg Kohn and Sham, that the transverse levels of parallel quantum wires can lock together under certain conditions. As a novel phenomenon, the effect of energy level locking deserves further study and should have interesting implications for experiments.

The purpose of this paper is to present a systematic theoretical study of the electronic structures of parallel quantum wires, with emphasis on the effect of energy level locking. The quantum wires we consider are of the Coulomb-confined type [9], and the calculations are performed self-consistently. In Sec. II, we review briefly the formalism of the Hohenberg-Kohn-Sham density functional theory, and its application to the present quantum wire system. In Sec. III, we present the results of calculations for two parallel quantum wires in different situations. In similar wires, the effect of energy level locking is found to be favored and the origin of the effect is charge transfer between the wires. In dissimilar wires, however, the electronic structure is quite different, and energy level locking is much less likely to occur. Energy level locking in similar wires remains strong for quite large wire separations, because the energy cost of the charge transfer depends logarithmically on the wire separation. But the effect of energy level locking is gradually suppressed by the tunneling between wires when the wire separation becomes small. In Sec. IV, we present a brief discussion of the experimental implications of these theoretical results.

The structure of the parallel quantum wires that we consider is shown in Fig. 1. Electrons are confined to the x-y plane, which may represent a semiconductor heterointerface. Two uniform positive ribbons A and B, representing regions of donors in a semiconductor heterostructure, extend infinitely in the y-direction, offset from the x-y plane by a distance d . The ribbons have widths of w_a and w_b , respectively, and a separation s . The whole system is charge-neutral, and is embedded in a uniform dielectric. The 2DEG has a uniform Fermi energy and is confined laterally by the self-consistent effective potential that includes the Coulomb interaction and the many-body effects of exchange and correlation.

II. DENSITY FUNCTIONAL THEORY

The Hohenberg-Kohn-Sham density functional theory [15,16] provides an accurate treatment of the effects of exchange and correlation for the ground state properties of inhomogeneous electron systems. In this theory, the effective Schrödinger equation for an electron of a 2DEG is

$$-\frac{\hbar^2}{2m^*} \left[\frac{d^2}{dx^2} + \frac{d^2}{dy^2} \right] \Psi_{\ell k}(x, y) + V_{eff}[n; x, y] \Psi_{\ell k}(x, y) = E_{\ell k} \Psi_{\ell k}(x, y), \quad (1)$$

where $\Psi_{\ell k}(x, y)$ and $E_{\ell k}$ are the eigenfunction and eigen energy, respectively. $V_{eff}[n; x, y]$ is the effective potential energy, which is a functional of the two-dimensional electron density $n(x, y)$. In the local density approximation,

$$V_{eff}[n; x, y] = V_C(x, y) + E'_{xc}[n] = V_C(x, y) + \frac{d}{dn}(n\varepsilon_{xc}[n]), \quad (2)$$

where V_C is the Coulomb energy and $\varepsilon_{xc} = \varepsilon_x + \varepsilon_c$, with ε_x and ε_c being the exchange and correlation energies per electron, respectively. For a 2DEG, the exchange energy ε_x has the following analytic form [17]

$$\varepsilon_x[n] = -\frac{8\sqrt{2}}{3\pi r_s} = -\frac{8a_0^*}{3\pi} \sqrt{2\pi n}, \quad (3)$$

where a_0^* is the effective Bohr radius. The correlation energy ε_c has been calculated numerically [18,19].

For the two parallel quantum wires shown in Fig. 1, the two-dimensional density of donors in the charged ribbons is described by

$$n_d(x) = \begin{cases} \sigma_a & \text{if } -s/2 - w_a < x < -s/2 \\ \sigma_b & \text{if } s/2 < x < s/2 + w_b \\ 0 & \text{otherwise} \end{cases} \quad (4)$$

Because the system is uniform in the y-direction, equation 1 reduces to the one-dimensional form

$$-\frac{\hbar^2}{2m^*} \frac{d^2}{dx^2} \Phi_\ell(x) + V_{eff}[n; x] \Phi_\ell(x) = E_\ell \Phi_\ell(x), \quad (5)$$

where

$$\Psi_{\ell k}(x, y) = \Phi_\ell(x) e^{iky}, E_{\ell k} = E_\ell + \frac{\hbar^2 k^2}{2m^*}. \quad (6)$$

In equations 5 and 6, $\Phi_\ell(x)$ and E_ℓ are the transverse eigenfunction and eigen energy, respectively, and k is the wave number in the y-direction. At zero temperature, the two-dimensional electron density $n(x)$ relates to the transverse wave functions through

$$n(x) = 2 \sum_{\ell k} |\Psi_{\ell k}(x, y)|^2 = \frac{2}{\pi} \sqrt{\frac{2m^*}{\hbar^2}} \sum_{\ell, E_\ell \leq E_F} \sqrt{E_F - E_\ell} |\Phi_\ell(x)|^2. \quad (7)$$

After performing the integral over x on both sides of equation 7, we obtain

$$N = \int_{-\infty}^{\infty} dx n(x) = \frac{2}{\pi} \sqrt{\frac{2m^*}{\hbar^2}} \sum_{\ell, E_\ell \leq E_F} \sqrt{E_F - E_\ell}, \quad (8)$$

where N is the linear electron density in the y-direction. Finally, choosing the potential at $x = \pm\infty$ to be zero, the Coulomb energy in equation 2 is given by

$$V_C(x) = \frac{e^2}{4\pi\epsilon_0\epsilon} \int_{-\infty}^{\infty} dx' \int_{-\infty}^{\infty} dy' \left\{ \frac{n(x')}{\sqrt{(x-x')^2 + y'^2}} - \frac{n_d(x')}{\sqrt{(x-x')^2 + y'^2 + d^2}} \right\}. \quad (9)$$

The inputs for the numerical calculations are the geometric parameters w_a , w_b , s , and d , and the donor densities σ_a and σ_b . Using equations 2, 5, 7, and 8, and 9, the transverse wavefunction $\Phi_\ell(x)$, transverse level E_ℓ , Fermi energy E_F , and electron density $n(x)$ were calculated self-consistently. In our calculations, we used the effective mass $m^*=0.067$ and the dielectric constant $\epsilon=12.5$, corresponding to the values for GaAs.

III. NUMERICAL RESULTS AND DISCUSSION

In this section, we present the self-consistent numerical results at zero temperature for two parallel quantum wires in different situations. The calculated electronic structures of similar and dissimilar parallel wires are presented in separate subsections, because their features are very different. Some qualitative analyses are made following the numerical results. A theoretical summary is given at the end of this section.

A. Similar parallel wires

The calculated electronic structure of two similar parallel quantum wires is shown in Fig. 2. The widths of wires are $w_a = 190$ nm and $w_b = 200$ nm, respectively. The other geometric parameters are $s = 200$ nm and $d = 20$ nm. The donor densities in the two charged ribbons are kept the same, $\sigma_a = \sigma_b = \sigma$. Since the system is charge-neutral overall, σ can also be regarded as an electron filling parameter. In Fig. 2, the solid lines are the six lowest transverse energy levels E_ℓ , and the dashed line is the Fermi energy E_F . The energy levels are labelled A or B, according to whether they belong primarily to wire A or B, respectively, as determined by inspection of the calculated eigenfunctions.

Notice that when the Fermi energy rises up through the lower of a pair of adjacent energy levels with increasing σ , the (algebraic) slope of the lower energy curve of the pair increases while that of the upper curve decreases. Thus the two corresponding energy levels are brought closer together. Levels 3 and 4 lock together at the Fermi energy, while the gap between levels 5 and 6 narrows by a factor of about 5. These effects are referred to as “energy level locking”. In Fig. 2, we observe three features that characterize energy level locking. The first is that the effect is associated with the Fermi energy crossing the corresponding levels. The second is that the locked levels tend to remain together. The third feature is that the sequence of locked levels remains unchanged throughout. (For the lockings in Fig. 2, the level belonging to wire B is always lower than the level belonging to wire A.)

The energy level locking is caused by a charge imbalance that occurs between the wires and modifies the Coulomb potentials when a transverse level begins to fill. The origin of the charge imbalance is the $E^{-1/2}$ density of states singularity at the bottom of a subband, characteristic of quasi-one-dimensional systems. Note that a transverse level E_ℓ corresponds to the bottom of subband $E_{\ell k}$, as reflected in equation 6. When the Fermi energy rises up through E_ℓ , because of the density of states singularity, most of the added electrons go into subband $E_{\ell k}$. Thus the wire to which E_ℓ mainly belongs acquires an excess of electrons, and a charge imbalance occurs. Such a charge imbalance, through the Coulomb interaction, shifts the self-consistent electrostatic potential and the transverse energy levels of the wire with the excess (deficiency) of electrons upwards (downwards) significantly, favoring energy level locking. Energy levels that lock together do not separate immediately when the Fermi energy rises above them, because their density of states singularities almost coincide, which inhibits further changes of the charge differential.

Some features of the electronic structure in Fig. 2 can be understood qualitatively as a competition between a charge imbalance and inter-wire quantum hybridization. The inter-wire quantum hybridization acts to separate the adjacent levels, and thus opposes energy level locking. In Fig. 2, the separations between levels 3 and 4 and between levels 5 and 6 narrow markedly when the Fermi energy crosses them. This implies that the charge imbalances are the dominant factor. However, the energy gap between levels 5 and 6 remains fairly large. This is because inter-wire quantum tunneling and therefore hybridization is more significant for higher levels. A charge imbalance occurring in a high level induces an electrostatic potential that acts like an external field on lower levels. Thus this charge imbalance can cause the corresponding pairs of lower levels to lock together or even anticross. In this way, in Fig. 2, when level 5 begins to fill, level 3 and 4 are brought together significantly. On the other hand, levels 1 and 2 anticross twice (indicated by the arrows), corresponding to the Fermi energy crossing level 5 and 6, respectively.

To show that a charge transfer does occur when a transverse level begins to fill, we present the following simple argument. Consider the situation where all populated levels are tightly

bound, so that the wavefunction overlaps between the different wires are negligible. Suppose when $\sigma = \sigma_0$, the Fermi energy is $E_F(\sigma_0) = E_3$, (see Fig. 3). According to equation 8, the ratio of the numbers of electrons in wires A and B is given by

$$r(\sigma_0) = \frac{N_a(\sigma_0)}{N_b(\sigma_0)} = \frac{\sqrt{E_F(\sigma_0) - E_2}}{\sqrt{E_F(\sigma_0) - E_1}}. \quad (10)$$

For simplicity, let us assume that the potentials remain unchanged although σ increases. In other words, the increase of E_F is completely caused by the increase of σ . Suppose that when σ increases from σ_0 by a small amount $\Delta\sigma$, E_F increases by a small amount ΔE so that E_F locates above level 3 but still below level 4. This situation is shown in Fig. 3. Then, at $\sigma = \sigma_0 + \Delta\sigma$, the electron linear densities in wires A and B are

$$N_a(\sigma_0 + \Delta\sigma) = N_a(\sigma_0) + \frac{1}{\pi} \sqrt{\frac{2m^*}{\hbar^2}} \frac{\Delta E}{\sqrt{E_F(\sigma_0) - E_2}} \quad (11)$$

and

$$N_b(\sigma_0 + \Delta\sigma) = N_b(\sigma_0) + \frac{1}{\pi} \sqrt{\frac{2m^*}{\hbar^2}} \frac{\Delta E}{\sqrt{E_F(\sigma_0) - E_1}} + \frac{2}{\pi} \sqrt{\frac{2m^*}{\hbar^2}} \sqrt{\Delta E}, \quad (12)$$

respectively. The last term in equation 12 is due to level 3. The other two terms containing ΔE in equations 11 and 12 are associated with the 2nd and 1st levels, respectively. Because ΔE is very small, the term due to level 3 in equation 12 dominates the other terms. Keeping to the lowest order in ΔE , r becomes

$$r(\sigma_0 + \Delta\sigma) = r(\sigma_0) - r(\sigma_0) \frac{\sqrt{\Delta E}}{\sqrt{E_F(\sigma_0) - E_1}}. \quad (13)$$

This equation implies that a charge imbalance occurs when a new level begins to fill.

If σ increases from σ_0 by $\Delta\sigma$ so that E_F rises above both levels 3 and 4, another term due to level 4 should be added to the expression of r

$$r(\sigma_0 + \Delta\sigma) = r(\sigma_0) - r(\sigma_0) \frac{\sqrt{\Delta E}}{\sqrt{E_F(\sigma_0) - E_1}} + r(\sigma_0) \frac{\sqrt{\Delta E'}}{\sqrt{E_F(\sigma_0) - E_2}}, \quad (14)$$

where $\Delta E' = E_F(\sigma_0 + \Delta\sigma) - E_4$. In similar parallel wires, because $E_1 \sim E_2$ and $E_3 \sim E_4$, the two terms in equation 14 tend to cancel each other. Because of this cancellation, when

σ increases, further differential charging is inhibited and thus the locked levels tend to stay together.

Obviously, the above argument also holds for situations when higher levels are crossed by the Fermi energy. In the self-consistent calculations, however, the electrostatic potentials and transverse levels are actually affected by the charge imbalance and move in response to it. (These electrostatic level shifts are in fact responsible for the energy level locking.) Because of this electrostatic response, the self-consistent charge imbalance is not as large as that given by equations 13 and 14. In Fig. 4, we display the calculated ratio r for the range of σ in which the Fermi energy crosses the 5th and 6th transverse levels. Notice that $r_0 = w_a/w_b = 0.95$ corresponds to perfect charge balance between the wires. Our calculation shows that r oscillates about r_0 ; its drop near $\sigma = 1.8 \times 10^{10} \text{ cm}^2$ and rise beginning at $\sigma = 2.0 \times 10^{10} \text{ cm}^2$ are due to the 5th and 6th transverse levels beginning to fill, respectively.

In Fig. 2, another feature of the electronic structure is that all transverse energy levels first decrease and then increase in energy while σ increases. This behavior results from the competition between the Coulomb energy and the exchange-correlation energy. According to equation 3, $\varepsilon_x \propto -n^{1/2}$. The correlation energy ε_c also increases negatively with n , but slower than ε_x . [18,19] The Coulomb energy has no strict power-law dependence on the electron density, because the electron density appears in the integral in equation 9. However, when all populated transverse levels are tightly bound, electrons distribute mainly within the potential wells and thus approximately $V_C \propto n$. At low electron densities, the exchange-correlation energy dominates the Coulomb energy. In fact, the exchange-correlation energy confines electrons so tightly that the Coulomb energy is overall positive. [9] Because the exchange-correlation energy dominates the Coulomb energy at low densities, increasing σ results in further lowering of all transverse levels. However, when the electron density is increased sufficiently, the Coulomb energy becomes more important, thus causing the energy curves to become flat and then to rise gradually.

The competition between the Coulomb energy and the exchange- correlation energy also

affects the energy level locking in an important way. According to equations 2 and 3, when there is a small increase of the electron density Δn , the variation of contribution from the exchange energy itself to the total effective potential energy is

$$\Delta E'_x = -\frac{4a_0^* \Delta n}{\sqrt{2\pi n}}. \quad (15)$$

However, $\Delta V_C \propto \Delta n$, that is, approximately independent of n . When n is extremely low, $\Delta E'_x$ may dominate ΔV_C . Then, since $\Delta E'_x$ differs in sign from ΔV_C , a charge imbalance will not result in energy level locking at extremely low densities. Therefore, energy level locking in similar wires also requires a sufficient electron density so that the Coulomb energy is dominant.

To study the role of inter-wire separation on energy level locking, we have calculated the electronic structure as a function of the wire separation s . The result is shown in Fig. 5. The parameters used were $w_a = 190$ nm, $w_b = 200$ nm, $d = 20$ nm, and $\sigma_a = \sigma_b = 2.0 \times 10^{10}$ cm², which are the locking of levels 5 and 6 in Fig. 2. The solid lines are the eight lowest levels and the dotted line is the Fermi energy. On the right side of this figure, the solid lines ending with solid circles and the dashed lines ending with open circles correspond to the energy levels of isolated wires A and B, respectively.

Compared to the gaps between corresponding levels of the isolated wires, we observe strong effects of energy level locking for large wire separation. When s is small, however, the inter-wire tunneling becomes strong, which causes the energy levels to become well separated because of hybridization. To illustrate the role of the tunnelling when s becomes small, we show in Fig. 6 the wave functions of the lowest four levels for a wire separation $s = 100$ nm. Notice that the widths of the electrostatically confined quantum wires are somewhat larger than the widths of the ribbons of positive charge that confine the electrons. In case shown there is significant tunneling between the wires and the higher energy wavefunctions have similar amplitudes in both wires. In Fig. 5, the lower pairs of levels show more tendency to lock together, because the electrons of low levels experience a higher barrier between wires. Finally, we should point out that levels 3 and 4 are closer than levels 1 and 2 for large

s , because, at this particular value of σ , the order of levels 1 and 2 is reversed (check the wavefunctions or refer to Fig. 2).

An interesting feature of Fig. 5 is that even for the large wire separation s of 800 nm, the gaps between the paired levels of the two interacting wires are still much smaller than the gaps between the corresponding levels of isolated wires. Thus the energy level locking found in the present model is a quite long-range effect. The reason for this is that the Coulomb energy cost of the charge transfer between infinite parallel wires depends logarithmically on the distance between the wires (for large s), and is thus insensitive to the wire spacing. On the other hand, the tunneling between wires that opposes the energy level locking decreases exponentially as s increases.

B. Dissimilar parallel wires

The electronic structures of dissimilar parallel quantum wires are quite different from those of similar parallel quantum wires. In Fig. 7, we present the calculated electronic structures for $w_a = 100$ nm and $w_b = 200$ nm. The other geometric parameters are $s = 200$ nm and $d = 20$ nm, and $\sigma_a = \sigma_b = \sigma$. The solid lines are the few lowest transverse energy levels, and the dotted line is the Fermi energy. The levels are again labelled A or B according to which wire they primarily belong to.

Generally speaking, in dissimilar parallel wires, the transverse levels of the two wires are well separated from each other. When the Fermi energy crosses a transverse level, an abrupt charge imbalance occurs for the same reason as in similar wires. The charge imbalance can significantly twist the curves of transverse levels, but is not sufficient to lock two levels together. The level twists are seen where the Fermi energy crosses the 3rd level in Fig. 7. However, if a pair of levels happen to be close when the Fermi energy crosses them, they can be squeezed together significantly by the charge imbalance. This is reflected in the crossing between levels 4 and 5 (indicated by an arrow). This energy crossing, however, is a case of “anticrossing” instead of level locking, because the level sequence reverses. The

anticrossing is associated with the asymmetry of the two wires. In this case, the charge imbalance narrows the energy gap at the anticrossing, but the levels then separate quickly.

Another way to study two dissimilar parallel wires is by varying the donor density of one wire, while fixing the donor density of the other wire. Such a case is shown in Fig. 8. Here, σ_b is varied while σ_a is fixed at $1.5 \times 10^{10} \text{ cm}^{-2}$. The parameters used here are $w_a = 190 \text{ nm}$, $w_b = 200 \text{ nm}$, $s = 200 \text{ nm}$, and $d = 20 \text{ nm}$. When σ_b increases, the Fermi energy also increases for the most part. To keep the Fermi energy the same in both wires, some electrons must transfer from wire B to wire A. These excess electrons cause wire A to have a net negative charge, and thus its energy levels rise with increasing σ_b . On the other hand, because wire B is deficient of electrons, its levels fall. Since the levels in wire A increase with the Fermi energy, their trajectories are similar to that of the Fermi energy. The Fermi energy is therefore unlikely to cross the levels of wire A. In other words, the Fermi energy can cross only one level at a time.

C. Summary

Based on above discussion, we summarize the conditions for energy level locking as follows.

- 1) The system should be quasi-one-dimensional and consist of parallel subsystems with Coulomb interaction.
- 2) The subsystems should be similar.
- 3) The electron density should not be too small.
- 4) The separation between the subsystems should be large enough for tunnelling between them to be weak.

It should be noted that the quasi-one-dimension condition is essential for energy level locking. To see this, let us consider a quasi-two-dimensional system, that is, an electron system that is confined in two quantum wells. Because there is no density of states singularity in the two-dimensional system, analogous to equation 12, we now have

$$\Delta N_b = \frac{m^*}{\pi \hbar^2} \sum_{\ell, E_\ell < E_F} \Delta E, \quad (16)$$

where ΔN_b is the variation of the area electron density in well B. This implies that all populated levels contribute to ΔN_b *equally*. The newly populated level does not have a dominant effect, and no significant charge imbalance is involved. Therefore, no energy level locking occurs in quasi-two-dimensional systems.

In quantum mechanical systems, the effect of “energy level anticrossing” is very common. Anticrossings occur because quantum hybridization between the sub-systems becomes important in near-degenerate situations. The hybridization opens an energy gap, lifting the incipient level degeneracy. Energy level locking is the opposite of anticrossing; i.e., instead of nearly degenerate energy levels “repelling” each other, they lock together. The characteristic differences between anticrossings and lockings are outlined in Table I.

In a particular system, level anticrossings and lockings may coexist. The resultant electronic structure depends on the competition between these two effects. In most situations, the effect of energy level locking is very weak. In the system of two parallel quantum wires, we have demonstrated by numerical calculations that the energy level locking can be the dominant effect.

IV. EXPERIMENTAL IMPLICATIONS

The theoretical results presented above are based on a specific model of quantum wires. The experimental realizations of quantum wires are more complicated systems, with the lateral confinement usually achieved by means of gates [20,21] rather than the ribbons of positive charge that we have considered here. However, the physical mechanism of level locking relies on the electronic density of states singularity that is common to all Fermionic parallel quantum wires, irrespective of the method of confinement. Another complication is that at present only short quantum wires (known as ballistic constrictions) are of sufficiently high quality for experimental studies of energy level locking to be feasible. In gated parallel constrictions [22,23], the electrons confined between the gates share the same Fermi energy

with the electron reservoirs of source and drain. A charge imbalance can be easily achieved by transferring electrons from or to the reservoirs. Moreover, the lateral confinement of electrons in the gated constrictions tends to be stronger than in the Coulomb-confined systems, so that the quantum hybridization that competes with level locking should be less important. Therefore, energy level locking may also occur in gated systems of similar parallel constrictions.

In a pioneering measurement for a gated system of two parallel constrictions, Smith *et al.* [22] found that the total conductance shows successive double steps of $4e^2/h$. The authors suggested that these double steps of conductance result from non-random alignments of the wire subbands. The $4e^2/h$ double steps have also been observed in measurements of other similar structures [24,25]. In a recent experimental study, however, Simpson *et al.* [23] compared the total conductance of two quantum constrictions to the sum of the two individual conductances, but found no evidence of simultaneous subband depopulation. Thus the experimental situation at present is unclear.

It is well-known [1,26,27] that, in an ideal one-dimensional system, the conductance is quantized, given by

$$G = \frac{2e^2}{h} N_p, \quad (17)$$

where N_p is the number of populated subbands. If energy level locking occurs in a gated system that contains two similar parallel constrictions, while tuning the gate voltage, the Fermi energy should cross a pair of transverse levels almost at the same time. (Notice that *exact* energy degeneracies do not occur in one-dimensional-systems. [28]) That is, N_p changes by 2 each time, and, therefore, G should show the double steps of $4e^2/h$.

One should note, however, that the curve of conductance vs gate voltage always has considerable sloping regions between adjacent plateaux. [26,27] If the sloping regions of the individual conductances corresponding to the two constrictions overlap partially, the total conductance of the system presents a double step as well. It turns out that there is a quite high probability that the total conductance shows a double step, even if the corresponding

levels associating with the two constrictions are well separated. Therefore, the occurrence of double steps in the total conductance curve does not necessarily mean that two transverse levels line up exactly.

Considering that one can now tune the gate voltages independently [23,29–31], we suggest another way to search experimentally for energy level locking. When one tunes one side gate voltage while fixing the other, the widths of plateaux of the total conductance also change. Based on our theoretical studies, we know that the locked levels tend to stay together. This feature should make the width of a plateau insensitive to the tuning gate voltage *when the plateau width is close to the maximum*. This is because the maximum width of the plateau corresponds to the smallest separation of the two levels, which is the situation of energy level locking. Experiments tuning one side gate voltage have been carried out by Simpson *et al.* [23] However, the voltage steps taken were too large for this test for energy level locking to be applied to the published data. Further experimental measurements would therefore be of interest.

Besides the transport properties, other measurements, such as the excitation spectrum, can also in principle be used to verify the existence of energy level locking in the parallel ballistic constrictions.

In conclusion, we have presented a theoretical study demonstrating that energy level locking should occur between similar parallel quantum wires. It is driven by a charge imbalance associated with the onset of filling of transverse energy levels with electrons. This novel phenomenon is qualitatively different from the anticrossing behavior that is typical of nearly degenerate energy levels in quantum systems. Our results should stimulate further experimental and theoretical studies of this phenomenon.

ACKNOWLEDGMENTS

We wish to thank D. Loss, M. Thewalt, and H. Trottier for stimulating discussions. This work was supported by the National Sciences and Engineering Research Council of Canada

and the Center for Systems Science at Simon Fraser University.

REFERENCES

- [1] For recent reviews see S. E. Ulloa, A. MacKinnon, E. Castaño, and G. Kirczenow, *From Ballistic Transport to Localization*, edited by P. T. Landsberg, Handbook of Semiconductors Vol. I (North-Holland, Amsterdam, 1992); C. W. J. Beenakker and H. van Houten, *Quantum Transport in Semiconductor Nanostructures*, edited by H. Ehrenreich and D. Turnbull, Solid State Physics, Advances in Research and Applications Vol. 44 (Academic Press, San Diego, 1991).
- [2] For a review, see M. L. Roukes, T. J. Thornton, A. Scherer, J. A. Simmons, B. P. van der Gaag, and E. D. Beebe, in *Science and Engineering of 1- and 0-Dimensional Semiconductors*, edited by S. P. Beaumont and C. M. Sotomayer-Torres (Plenum, London, 1990).
- [3] W. Y. Lai and S. Das Sarma, Phys. Rev. **B33**, 8874 (1986).
- [4] S. E. Laux and F. Stern, Appl. Phys. Lett. **49**, 91 (1986).
- [5] S. E. Laux, D. J. Franck, and F. Stern, Surf. Sci. **196**, 101 (1988).
- [6] J. H. Davies, Semicond. Sci. Technol. **3**, 995 (1988).
- [7] L. I. Glazman and I. A. Larkin, Superlatt. Microstruct. **6**, 32 (1988).
- [8] A. Nakamura and A. Okiji, J. Phys. Soc. Jpn. **60**, 1873 (1991).
- [9] Y. Sun and G. Kirczenow, Phys. Rev. **B47**, 4413 (1993).
- [10] Y. Avishai, M. Kaveh, S. Shatz, and Y. B. Band, J. Phys.: Condens. Matter **1**, 6907 (1989).
- [11] E. Castaño and G. Kirczenow, Phys. Rev. **B41**, 5055 (1990).
- [12] Y. M. Sirenko, P. Vasilopoulos, and I. I. Boiko, Phys. Rev. **B44**, 10724 (1991); H. C. Tso and P. Vasilopoulos, Phys. Rev. **B45**, 1333 (1992); I. I. Boiko, P. Vasilopoulos, and V. I. Sheka, Phys. Rev. **B45**, 135724 (1992).

- [13] U. Ravaioli, T. Kerkhoven, M. Raschke, and A. T. Galick, *Superlatt. Microstruc.* **11**, 343 (1992).
- [14] A preliminary account of part of this work has already been published. See Y. Sun and G. Kirczenow, *Phys. Rev. Lett.* **72**, 2450 (1994).
- [15] P. Hohenberg and W. Kohn, *Phys. Rev.* **136**, B864 (1964).
- [16] W. Kohn and L. J. Sham, *Phys. Rev.* **140**, A1133 (1965).
- [17] F. Stern, *Phys. Rev. Lett.* **30**, 278 (1973).
- [18] M. Jonson, *J. Phys.* **C9**, 3055 (1976).
- [19] B. Tanatar and D. M. Ceperly, *Phys. Rev.* **B39**, 5005 (1989).
- [20] T. J. Thornton, M. Pepper, H. Ahmed, D. Andrews, and G. J. Davies, *Phys. Rev. Lett.* **56**, 1198 (1986).
- [21] H. Z. Zhang, H. P. Wei, D. C. Tsui, and G. Weimann, *Phys. Rev.* **B34**, 5635 (1986).
- [22] C. G. Smith, M. Pepper, R. Newbury, H. Ahmed, D. G. Hasko, D. C. Peacock, J. E. F. Frost, D. A. Ritchie, G. A. C. Jones, and G. Hill, *J. Phys.: Condens. Matter* **1**, 6763 (1989).
- [23] P. J. Simpson, D. R. Mace, C. J. B. Ford, I. Zailer, M. Pepper, D. A. Ritchie, J. E. F. Frost, M. P. Grimshaw, and G. A. C. Jones, *Appl. Phys. Lett.* **63**, 3191 (1993).
- [24] S. W. Hwang, J. A. Simmons, D. C. Tsui, and M. Shayegan, *Phys. Rev.* **44**, 13497 (1991).
- [25] P. E. Schmidt, M. Okada, K. Kosemura, and N. Yokoyama, *Jpn. J. Appl. Phys.* **30**, L1921 (1991).
- [26] B. J. van Wees, H. van Houten, C. W. J. Beenakker, J. G. Williamson, L. P. Kouwenhoven, D. van der Marel, and C. T. Foxon, *Phys. Rev. Lett.* **60**, 848 (1988).

- [27] D. A. Wharam, T. J. Thornton, R. Newbury, M. Pepper, H. Ahmed, J. E. F. Frost, D. G. Hasko, D. C. Peacock, D. A. Ritchie, and G. A. C. Jones, *J. Phys. C: Solid State Phys.* **21**, L209 (1988).
- [28] In one-dimensional quantum systems, exact energy level degeneracies do not occur. See L. D. Landau, E. M. Lifshitz and L. P. Pitaevskii, *Quantum Mechanics, Non-Relativistic Theory* (Pergamon, New York, 1986), 3rd ed., Sec. 21.
- [29] Y. Feng, A. S. Sachrajda, R. P. Taylor, J. A. Adams, M. Davies, P. Zawadzki, P. T. Coleridge, D. Landheer, P. A. Marshall, and R. Barber, *Appl. Phys. Lett.* **63**, 1666 (1993).
- [30] R. P. Taylor, J. A. Adams, M. Davies, P. A. Marshall, and R. Barber, *J. Vac. Sci. Technol.* **B11**, 628 (1993).
- [31] S. Yang, M. J. Berry, A. S. Adourian, R. M. Westervelt, and A. C. Gossard, *Bull. Am. Phys. Soc.* **37**, 70 (1994).

FIGURES

FIG. 1. Schematic drawing of two parallel Coulomb-confined quantum wires.

FIG. 2. The calculated transverse energy levels of two similar parallel quantum wires (solid lines) and Fermi energy (dotted line) vs the uniform donor density σ . Energy levels are labelled A and B according to which wire they belong principally to. Arrows indicate anticrossings. Model parameters are $w_a = 190$ nm, $w_b = 200$ nm, $s = 200$ nm, and $d = 20$ nm.

FIG. 3. Schematic energy level structure of a pair of parallel wires. The horizontal axis is the longitudinal wave vector k and the vertical axis is the subband energy E_{lk} . The parabolic curves are the four lowest subbands. Level 3 is filled while level 4 is empty.

FIG. 4. Calculated electron number ratio r between the wires. $r_0 = w_a/w_b = 0.95$ corresponds to perfect charge balance. The solid line is a guide to the eye.

FIG. 5. Energy levels (solid lines) and Fermi energy (dotted line) vs the inter-wire separation s . Parameters are $w_a = 190$ nm, $w_b = 200$ nm, $d = 20$ nm, and $\sigma_a = \sigma_b = 2.0 \times 10^{10}$ cm². The right side solid lines and the dashed lines correspond to the energy levels of isolated wire A and B, respectively.

FIG. 6. Wavefunctions of the four lowest levels when $s = 100$ nm. Other parameters are the same as those in Fig. 5.

FIG. 7. The electronic structures of dissimilar parallel quantum wires. $w_a = 100$ nm and $w_b = 200$ nm, and other parameters are $s = 200$ nm and $d = 20$ nm. The levels are labelled A or B according to which wire they primarily belong to.

FIG. 8. σ_b is varied while σ_a is fixed at 1.5×10^{10} cm². The parameters are $w_a = 190$ nm, $w_b = 200$ nm, $s = 200$ nm, and $d = 20$ nm. Levels are labelled A or B according to which wire they primarily belong to.

TABLES

TABLE I. A comparison of the characteristic differences between anticrossings and lockings.

Anticrossings	Lockings
single-particle effect	many-particle effect
opening a gap	reducing the gap
caused by wave function overlap	caused by a charge imbalance
level sequence switches	no level sequence switches
occurs in all dimension	occurs in one dimension

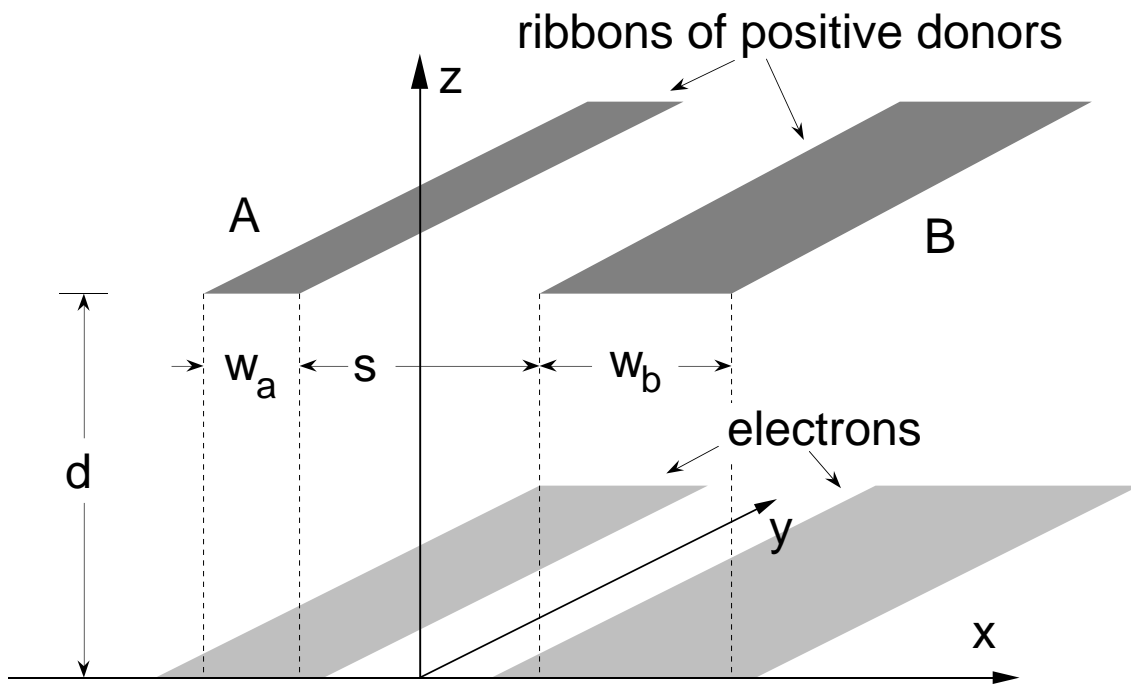


Figure 1

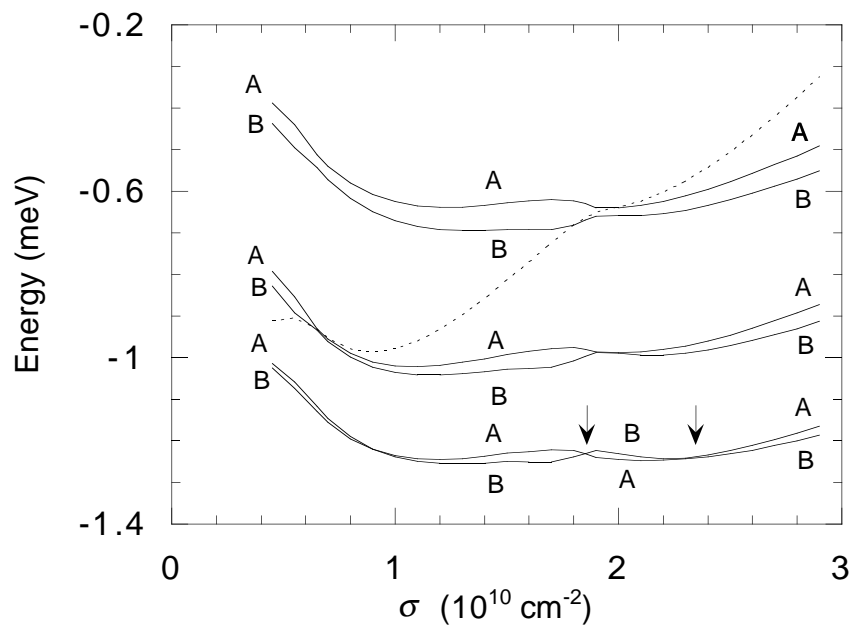


Figure 2

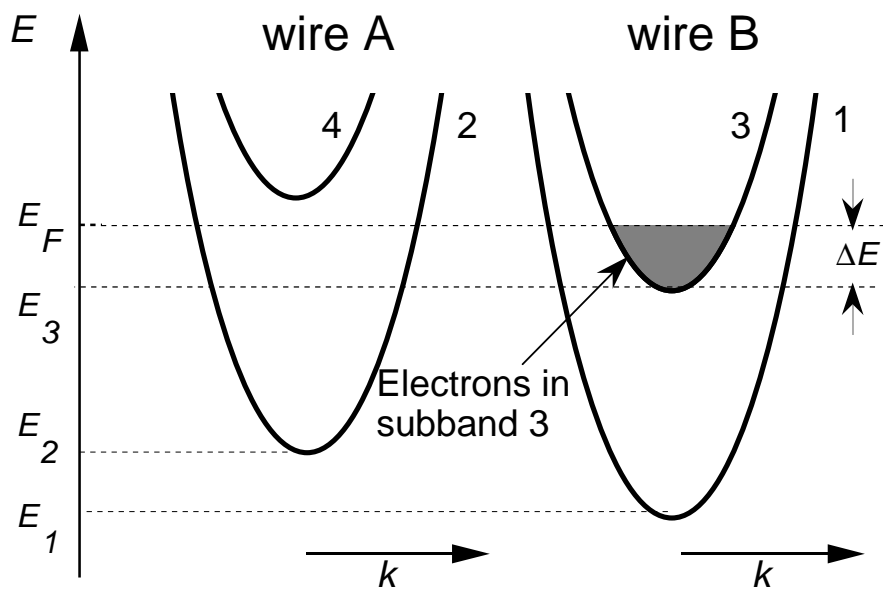


Figure 3

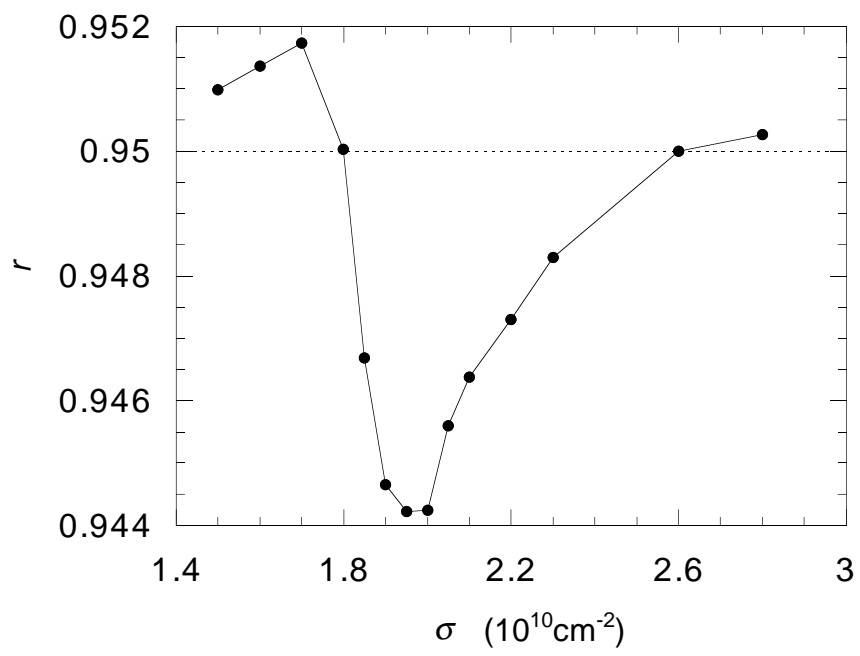


Figure 4

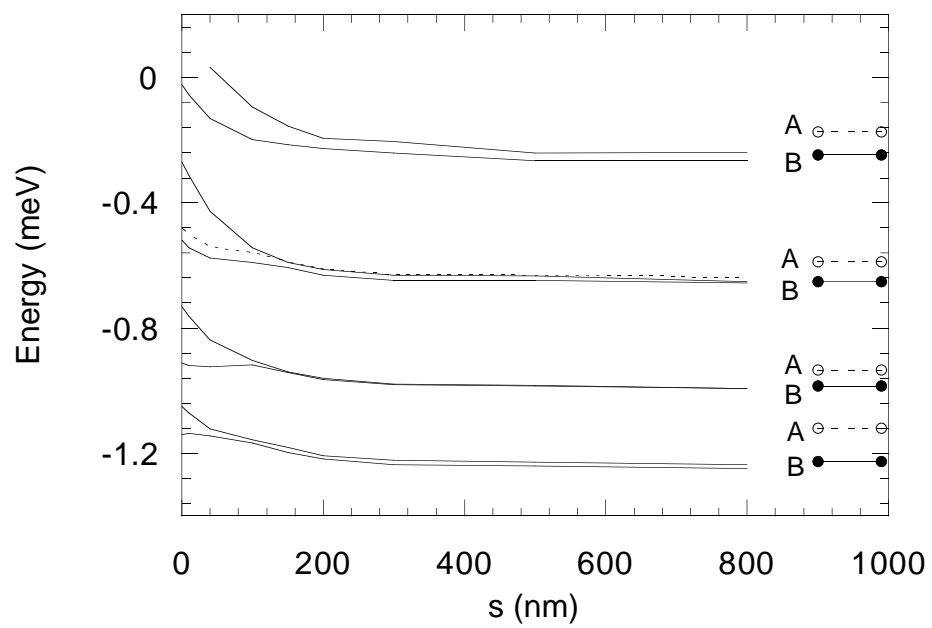


Figure 5

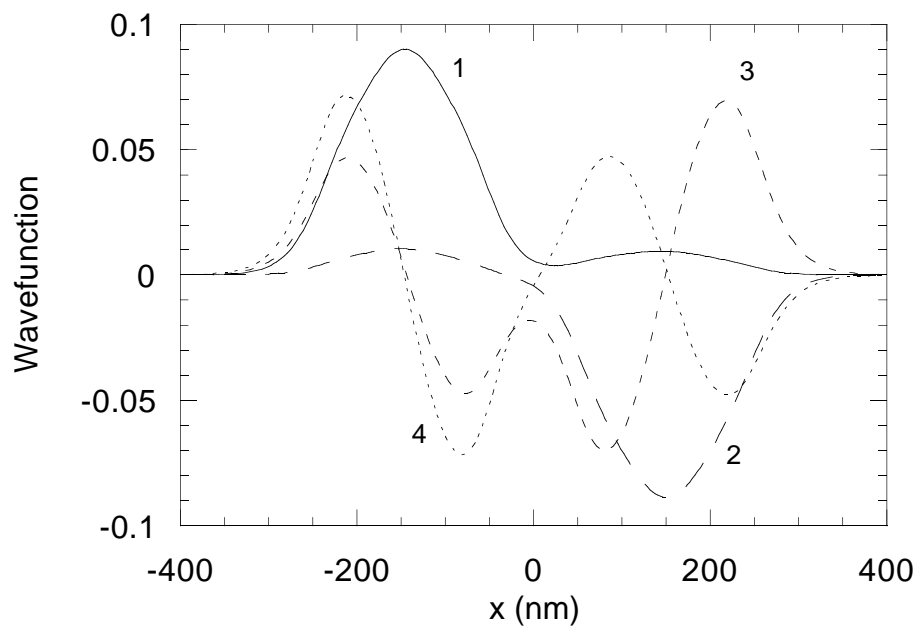


Figure 6

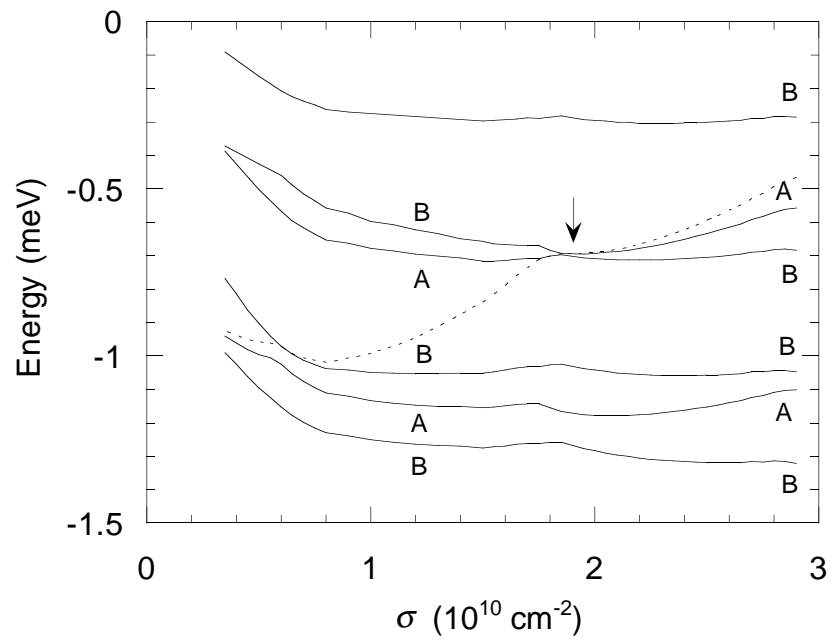


Figure 7

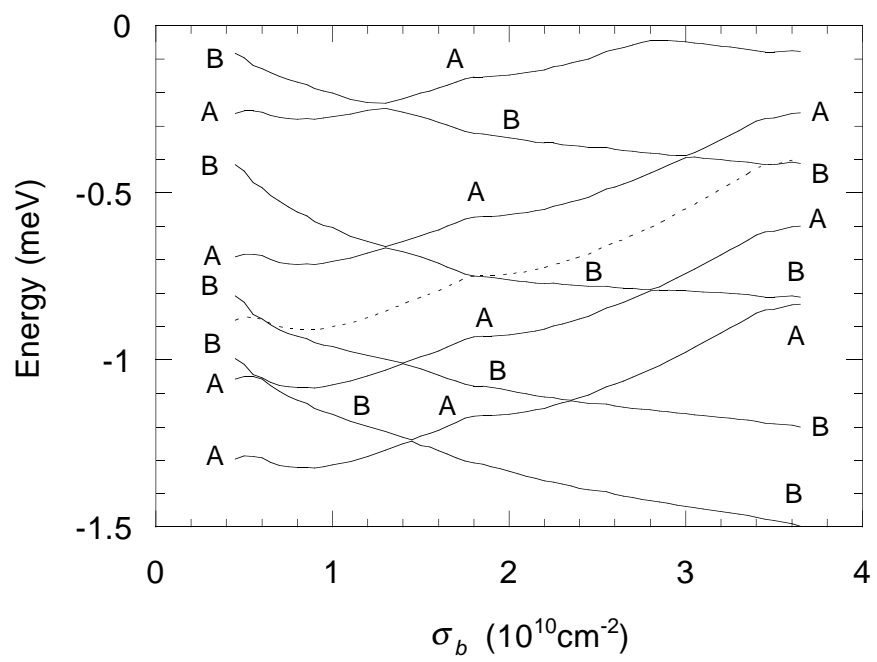


Figure 8